[59] R. E. Matick, "Review of current proposed technologies for mass storage systems," *Proc. IEEE*, vol. 60, pp. 266–289, Mar. 1972.
[60] D. O. Sproule and H. J. Hughes, U.K. Patent 604 429, July 5, 1948.
[61] T. Van Duzer, "Novel system for broadband focussing and guiding of acoustic surface waves," presented at the Solid State Device Conf., University of Rochester, Rochester, N. Y., June 25, 1969, Paper 15.
[62] E. Stern, "Microsound components, circuits and applications," *IEEE Trans. Microwave Theory Tech. (Special Issue on Microwave Acoustics)*, vol. MTT-17, pp. 835–844, Nov. 1969.
[63] I. M. Mason, "Anisotropy, diffracting scaling, surface wave lenses and focussing," *J. Acoust. Soc. Amer.*, to be published.
[64] W. C. Wang, "Signal generation via nonlinear interaction of oppositely directed sonic waves in piezoelectric semiconductors," *Appl. Phys. Lett.*, vol. 18, pp. 337–338, 1971.
[65] C. W. Turner, I. M. Mason, and J. Chambers, "Acoustic convolution using nonlinear surface wave interactions in a piezoelectric semiconductor," *Electron. Lett.*, vol. 7, pp. 696–697, 1971.
[66] R. L. Gunshor and C. W. Lee, "Generation of surface acoustic wave correlation echo from coupling to charge carries," *Appl. Phys. Lett.*, vol. 21, no. 1, pp. 11–12, 1972.
[67] M. Luukkala and J. Surakka, "Acoustic convolution and correlation and the associated nonlinearity parameters in $LiNbO_3$," *J. Appl. Phys.*, vol. 43, no. 6, pp. 2510–2518, 1972.
[68] F. G. Marshall, E. G. S. Paige, and A. S. Young, "New unidirectional transducer and broadband reflector of acoustic surface waves," *Electron. Lett.*, vol. 7, pp. 638–640, 1971.
[69] L. Kuhn, M. L. Dakss, P. F. Heidrich, and B. A. Scott, "Deflection of an optical guided wave by a surface acoustic wave," *Appl. Phys. Lett.*, pp. 265–267, Sept. 15, 1970.
[70] L. Kuhn, P. F. Heidrich, and E. G. Lean, "Optical guided wave mode conversion by an acoustic surface wave," *Appl. Phys. Lett.*, pp. 428–430, Nov. 15, 1971.
[71] F. R. Gfeller and C. W. Pitt, "Colinear acousto-optic deflection in thin films," *Electron. Lett.*, to be published.

Acoustic Surface-Wave Recirculating Memory

H. VAN DE VAART AND L. R. SCHISSLER

Invited Paper

Abstract—**An acoustic surface-wave memory is described, operating at a bit rate of 220 MHz and storage capacity of 1280 bit per recirculation loop. The transducers are coded using orthogonal pairs of Golay complementary sequences to obtain pulse-in pulse-out behavior. The shape of the delayed pulse is analyzed and compared with the pulse shape that is obtained using a simple single finger pair transducer. The recirculation electronics uses standard MECL-III logic for both the amplifier and the write, read, inhibit, and reclocking functions. The cost of the recirculating memory and the feasibility of constructing larger capacity stores are also discussed.**

I. Introduction

ULTRASONIC delay lines have been used in recent years in two modes of operation. The first one is the analog mode, in which an RF signal is either pulse, frequency, or phase modulated and delayed or temporarily stored for later signal processing such as correlation. The other is the digital mode, in which a series of pulses, representing digital data, are stored in temporary memories such as are used in graphics storage, desk calculators, etc. In the latter application, video pulses are inserted into a delay line, and when they emerge at the output are amplified and inserted back into the delay line, thus forming a recirculating loop. In this paper, we will be concerned with the digital application, using acoustic surface waves.

The basic recirculating memory has the configuration as shown in Fig. 1. Binary data are fed into the loop through the "write" gate. The new data are then amplified in the delay line driver (this step may not be necessary, depending on the voltage levels in the circuitry and delay line insertion loss)

Manuscript received April 20, 1972; revised September 13, 1972.
The authors are with the Sperry Rand Research Center, Sudbury, Mass. 01776.

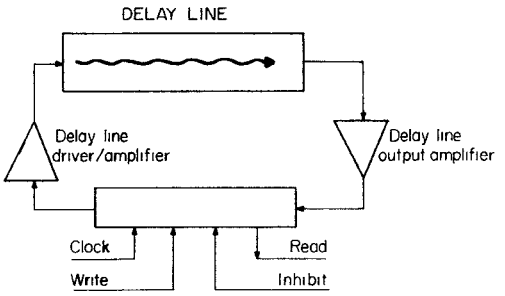

Fig. 1. Basic recirculating memory.

and fed into the delay line. At the output of the delay line, the pulses are amplified back up to logic level and retimed with respect to a continuously applied clock signal to correct for small delay time variations. The data can also be read out at the output of the amplifier without disturbing recirculation. An inhibit signal interrupts the recirculation when new data are to be inserted into the loop.

There are obviously many considerations that go into the design of a recirculating memory, and each design will always be a compromise between many factors, such as short latency time (the time that elapses before a given bit emerges at the output), large storage capacity, convenient frequency of operation, and, above all, the intended application and the cost of the memory [1], [2]. In the past, delay lines for digital storage were designed for maximum storage capacity in order to minimize the cost of access circuitry. Capacities of up to 20 000 bit have been reported at a frequency of a few megahertz, but with long latency time and large size [3], [4]. More recent considerations have indicated an optimum design that

uses a bit rate of 100 MHz and a capacity of ~1000 bit per storage loop, using bulk wave delay lines [5]–[9].

The maximum storage capacity of an acoustic delay line recirculating memory is dependent on the length of the line and the frequency of operation and is simply given by $N=F\times T$, where N is the number of stored bits, F is the bit rate, and T the delay time of the line. Thus, the larger the line and the higher the frequency, the larger the capacity. However, increasing the length of the line increases the latency time, which is equal to the total delay time. The average latency time is half that value.

A large storage density can be obtained when the bit rate is increased to as high a rate as is technically feasible. As it turns out, the limiting factor here is not the delay line part of the recirculation loop, but the electronic circuitry needed for reclocking, data insertion, etc. Surface-wave delay line transducers can be fabricated for frequencies up to 800 MHz using standard photoresist techniques, and even beyond that using electron-beam photoresist exposure techniques [10]. However, the highest speed integrated logic available is MECL-III, which is limited to ~300 MHz. Using discrete components instead of integrated logic, speeds up to 1 GHz seem feasible, but only at a very high manufacturing and component cost. For the memory to be described here, MECL-III logic was used, and the bit rate chosen was 220 MHz.

In the surface-wave approach to be discussed here, no detailed study has been made of the optimum design of the complete memory. Assuming equal bit rate and equal insertion loss for the same length delay line, electronic circuitry requirements will be similar, whether bulk wave delay lines or surface-wave delay lines are used. However, it is felt that the surface-wave approach leads to easier and more economical fabrication of the delay line portion of the store and lends itself to batch fabrication of many delay channels with exactly identical delay time and performance. Above all, the surface-wave technique is compatible with integrated circuitry techniques and allows easier integration of storage medium and electronic circuitry.

In this paper, we will report on the design and operation of a 220-MHz acoustic surface-wave recirculating memory using orthogonal pairs of Golay complementary sequences [11], [12] with a bit capacity of 1280 bit per recirculation loop. This bit capacity permits easy hookup to a high-speed 16-bit word generator for testing purposes and requires ~1 in of delay material, which can be readily obtained. In Section II, we will discuss the delay line part of the store, such as design of the transducer, substrate material, and the results predicted by the equivalent circuit analysis. These are then compared with the experimental results. Excellent agreement in regard to insertion loss and pulse distortion is obtained. In Section III, the electronics and layout of the recirculation part are described. The logic circuitry was kept as simple as possible and was intended to read the data in and out serially only. In the concluding section, possible improvements in the design of the memory will be discussed, as well as the feasibility of constructing larger capacity ultrasonic surface-wave memories and the factors that determine the cost per bit of the memory.

II. Design of the Surface-Wave Transducer

As is well known, the standard surface-wave interdigital transducer has a passband response centered around a center frequency and zero output at dc. Hence, a single pulse applied at the input of the delay line will emerge at the output in distorted form due to the limited bandwidth. In order to maximize the bandwidth of the transducer, the number of interdigital finger pairs must be as small as possible. Consequently, the simplest way to implement a video delay line is to use input and output transducers each consisting of one single finger pair. However, a simple analysis will show that this approach leads to unreasonable transducer requirements.

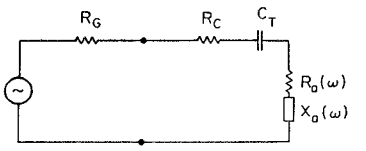

Fig. 2. Equivalent series circuit of surface-wave transducer.

According to Smith *et al.* [13], the interdigital transducer can be represented by a series circuit consisting of the transducer capacitance C_T, a radiation resistance $R_a(\omega)$, and an acoustic reactance $X_a(\omega)$, Fig. 2. At acoustic synchronism ω_0, $X_a(\omega_0)=0$ and $R_a(\omega_0)=(4/\pi)k^2N(1/\omega_0C_T)$, where k is the electromechanical coupling constant and N is the number of interdigital periods. Assuming for the moment zero resistance in the aluminum fingers, the insertion loss is given by

$$IL=\left[\frac{\left\{\omega_0C_TR_G+\frac{4}{\pi}k^2N\right\}^2+1}{2\left(\frac{4}{\pi}k^2N\right)\omega_0C_TR_G}\right]^2 \tag{1}$$

where R_G is the generator and load resistance. Minimum insertion loss is obtained when the transducer capacitance is adjusted such that

$$\omega_0C_T=\frac{1}{R_G}\sqrt{\left(\frac{4}{\pi}k^2N\right)^2+1}. \tag{2}$$

The insertion loss is then

$$IL=\left[1+\sqrt{1+\frac{1}{\left(\frac{4}{\pi}k^2N\right)^2}}\right]^2. \tag{3}$$

For $(4/\pi)k^2N\ll 1$, these expressions reduce to

$$\omega_0C_T=\frac{1}{R_G} \tag{4}$$

and

$$IL=\left(\frac{4}{\pi}k^2N\right)^{-2}. \tag{5}$$

For a single finger pair, $N=\frac{1}{2}$ and the quantity $(4/\pi)k^2N$ equals ~0.03 for $LiNbO_3$ and ~0.001 for quartz. Using (5), we find that for $LiNbO_3$ the minimum insertion loss $IL=30$ dB, while for quartz $IL=57$ dB.

Using (4), we can now calculate the transducer capacitance required to obtain minimum insertion loss. Assuming a generator and load impedance of 50 Ω and an operating frequency of 220 MHz, we find $C_T=14.5$ pF. Using Engan's expression [14] for the capacitance of a pair of strips on a dielectric substrate, we find that the length of the single finger pair transducer must be 4.5 cm for $LiNbO_3$ and 32 cm for quartz! It is obvious at this point that using a single finger pair as a video

pulse transducer is the wrong approach; not only is the required finger overlap too large, but the resistive losses of the aluminum fingers will become excessive. For instance, with a resistivity of 4.8×10^{-6} $\Omega\cdot$cm and an electrode thickness of 4000 Å, we obtain a resistance of $\sim300\,\Omega$ per centimeter finger length. It is clear that this will result in a large insertion loss.

The preceding simplified analysis could have been performed more exactly by assuming a nonzero transducer resistance R_c from the start and including the dependence of R_c on C_T. The analysis then becomes more complicated, but does not yield any new results. Reducing the finger length reduces R_c, resulting in a lower insertion loss, but at the same time increases the capacitive reactance, resulting in a higher insertion loss.

Reducing the finger overlap also increases the diffraction loss; but, for a few microseconds delay, the diffraction contributes less than 1 dB loss on either quartz or $LiNbO_3$ [15]. For time delays in the order of several tens of microseconds, diffraction loss contributes an appreciable portion of the total loss incurred and cannot be neglected. In that case, attenuation and possible beam steering loss must also be included in the determination of the overall insertion loss.

An alternate and superior approach in designing a transducer with pulse-in pulse-out behavior is to use binary phase-reversal codes [12], [16]. Here, the input transducer generates a phase coded acoustic signal which propagates to the output transducer, where the autocorrelation output is obtained. The advantage of this method is that the transducer consists of many finger pairs, all connected in parallel, resulting in a low R_c. Hence, the length of the code and the finger overlap length can be chosen to satisfy (2).

For nonperiodic biphase sequences, the correlation output consists of a central peak and a series of sidelobes. It is obviously important to make the central-peak-to-sidelobe ratio as large as possible. Well-known examples of such a sequence are the Barker codes; they have a central peak of height N, where N is the number of bits in the code, and a sidelobe level of height unity. The sidelobes can be eliminated altogether by using a pair of sequences which have the property that the sum of the correlation functions is zero except for the correlation peak. These are known as Golay or complementary sequences. Implementation of such sequences requires two acoustic propagation paths for a single information path, which is a disadvantage in the case of video delay lines where high storage density is important. This can be alleviated by using a second Golay pair, with the property that the sum of the cross correlations of the two pairs is zero for all time shifts. The second Golay pair can then be placed in the acoustic propagation path of the first Golay pair, thus restoring the original storage density. Such a set of complementary sequence pairs is known as a cooperative set. This principle can be generalized to N-path cooperative codes. However, no increase in storage density can be gained above the 2-pair cooperative set.

Several procedures have been reported in the literature to find suitable codes of various lengths [11], [12]. It is important to keep in mind that transducers using these codes all have the same property: they simulate the behavior of a transducer consisting of a single tap. In other words, if each coded transducer tap consists of one single finger pair, the overall output of the transducer is equal to a single finger pair; if each transducer tap consists of N finger pairs, the overall output of the transducer is equal to a transducer consisting of N finger pairs. Similarly, the bandwidths of the simple transducer and its phase coded equivalent are equal, and no reduction in insertion loss is to be expected from the latter, compared to the idealized case just discussed. The primary reason for the phase coding is the flexibility to adjust both the finger overlap and the length of the code for minimum insertion loss, at the same time greatly reducing the resistive finger losses.

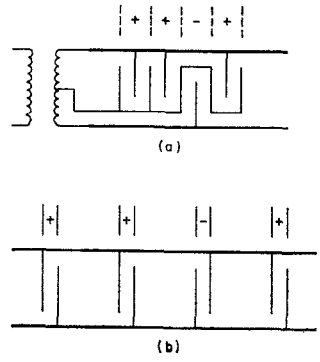

Fig. 3. Surface-wave transducer electrode structures used for complementary sequence coding.

A transducer specifically designed for pulse-in pulse-out behavior was developed by Whitehouse *et al.* [11], [16]. It is the so-called field delineated transducer, which uses a meandering groundline to separate the 0° and 180° taps, Fig. 3(a). Each tap consists of two finger pairs instead of one, but the time response, as will be shown in the following paragraphs, is still acceptable. However, the input and output are double ended, and the transducer must be driven by coincident positive and negative pulses.

A much simpler design was used by Tseng [12], Fig. 3(b). By placing the transducer taps several wavelengths apart, the field between two 0° taps (or two 180° taps) is small compared to the field between an interdigital finger pair. Hence, no meandering ground line is necessary to separate equal phase finger pairs; input and output are single ended.

Since the field delineated transducer simulates a transducer consisting of one periodic section, while the Tseng transducer is equivalent to a single finger pair, it is useful to compare the frequency and time responses of both the one periodic section and the single finger pair transducers. These have been computed using the transfer matrix to obtain the frequency responses and an FFT routine to obtain the corresponding time responses [17], [18]. The results are shown in Fig. 4. As can be seen, the frequency response of the one periodic section transducer is somewhat narrower than for the single finger pair transducer, and as a result a positive sidelobe shows up in the time-domain response. This sidelobe has an amplitude which is nearly one fifth the main peak amplitude and is separated from the main peak by exactly one bit period. This reduces the detection margin when a series of pulses is transmitted and is clearly undesirable.[1] Hence, we conclude that the single finger pair transducer has a superior time response compared to the one periodic section transducer.

[1] A more detailed discussion on detection margin and the factors affecting it can be found in [7].

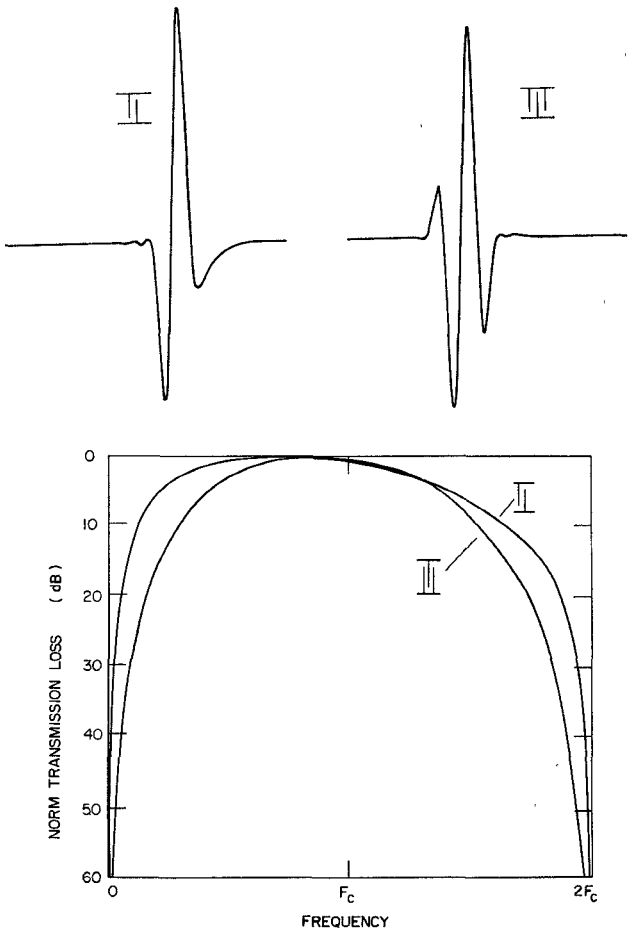

Fig. 4. Frequency and time responses of a set of transducers, consisting of one single finger pair each and one periodic section each. Frequency response curves are normalized to 0 dB.

The frequency and time responses shown in Fig. 4 were computed assuming $\omega_0 C_T R_G = 1$. In this case, the capacitive impedance is large compared to the radiation impedance, and the maximum in the transmission gain curve of Fig. 4 occurs below the acoustic synchronism frequency. Thus the frequency response is asymmetric, which results in an asymmetric time response. This is true for both quartz and $LiNbO_3$, and transducers for which the finger overlap is chosen to satisfy the relation $\omega_0 C_T R_G = 1$ will give an asymmetric time response on both those substrates. The shape can be made symmetric by deliberately mismatching the transducer from the generator and load impedance, but only at a cost of increased insertion loss.

The transducer design for the recirculating memory is shown in Fig. 5. It uses 16-bit cooperative sequences, with a single finger pair per tap. The finger width is 4 μ, with a center-to-center spacing of 8 μ, resulting in an acoustic synchronism frequency of 218 MHz. Input and output transducers were placed 2 cm apart, giving a storage capacity of 1250 bit per loop. To facilitate testing with a 16-bit word generator, the capacity was increased to 1280 bit (80×16) or a bit rate of 223 MHz. The finger overlap was 0.24 cm, yielding a total storage capacity of $\sim$10 000 bit/in^2.

The computed time response for this transducer on $LiNbO_3$ is shown in Fig. 6. The left two traces show the autocorrelation

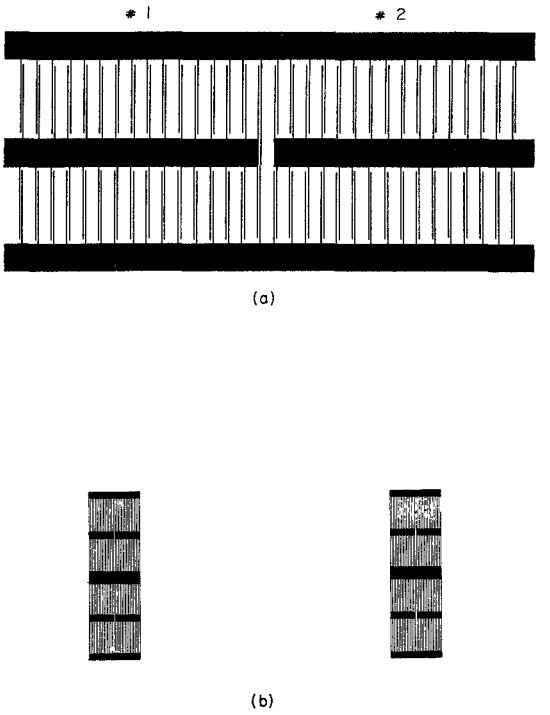

Fig. 5. Transducer design for surface-wave recirculating memory using two 16-bit cooperative sequences (a) and complete 4-channel delay line layout (b).

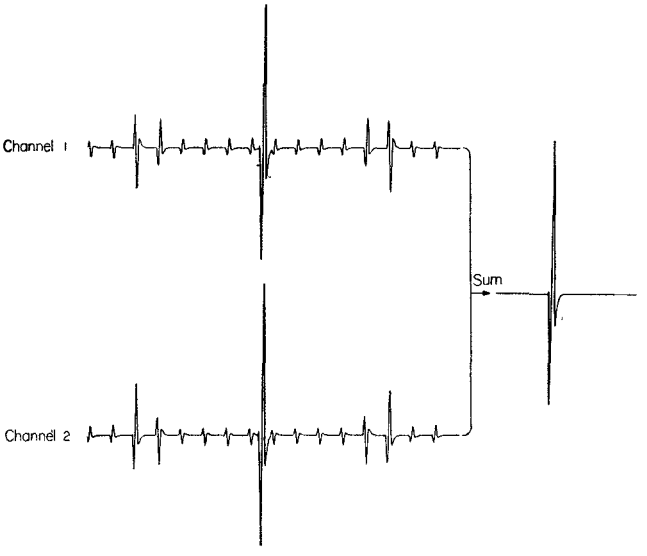

Fig. 6. Computed autocorrelation response of a 16-bit Golay coded transducer (number 1 in Fig. 5) on $LiNbO_3$.

responses of the Golay pair; the right side is the sum of the two responses. The finger overlap was chosen such that $\omega_0 C_T R_G \approx 1$, and thus the response is exactly the same as the response of the single finger pair as shown in Fig. 4. If the same transducer pattern design is used with quartz as the substrate, then, due to the lower dielectric constants of quartz, $\omega_0 C_T R_G \approx 0.1$. The capacitive impedance is now much higher, and we have essentially mismatched the transducer with respect to the generator and load impedances. The result is a somewhat higher insertion loss than the theoretical minimum, but also a symmetrical

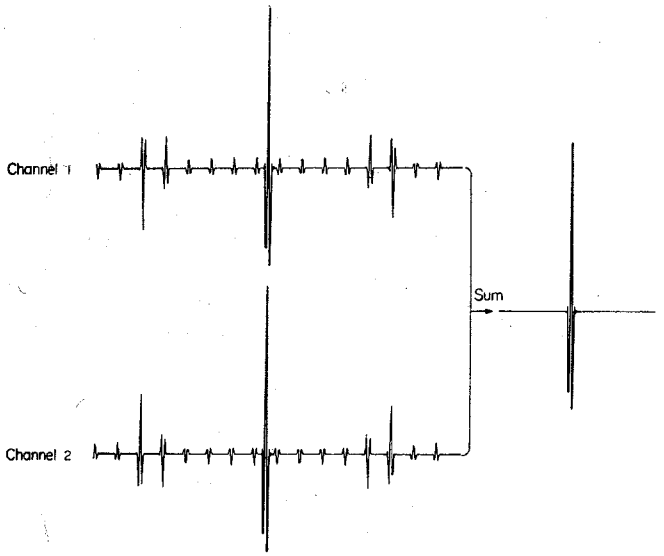

Fig. 7. Same as Fig. 6, except substrate material is quartz.

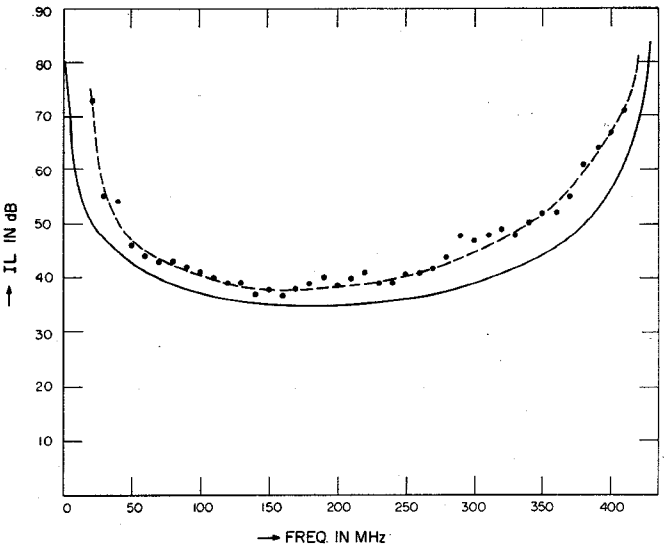

Fig. 8. Insertion loss versus frequency for 16-bit Golay coded transducer. Solid curve shows computed insertion loss using equivalent circuit model. Dots are measured values.

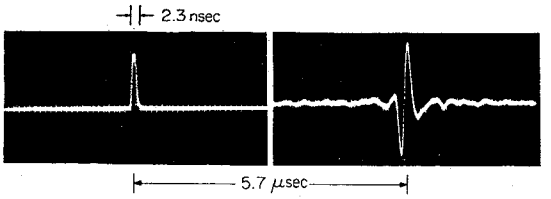

Fig. 9. Input pulse and delayed pulse for one channel of transducer shown in Fig. 5(b). Input pulse and output pulse (peak to peak) width: 2.3 ns.

delayed pulse as a result of the symmetrical frequency response. This is shown in Fig. 7. If the finger overlap had been adjusted so that the condition $\omega_0 C_T R_G = 1$ had been satisfied for quartz as the substrate, then the time-domain response would have been equal to that of $LiNbO_3$, just as in the case of the uncoded transducers discussed before. However, for the same transducer pattern design, the impulse responses on quartz and $LiNbO_3$ will be equal only when the transducer is mismatched on both substrates. This was apparently the case reported in [11]. Finally, the computed minimum insertion losses for the Golay coded transducer under the condition $\omega_0 C_T R_G = 1$ are identical to those computed for the single finger pair: 30 dB for $LiNbO_3$ and 57 dB for quartz.

An important consideration in the design of a recirculating memory is the cost. As will be shown later, the dominant part of the cost is in the electronic circuitry which forms the recirculation loop. The amplifier is the most critical part of the loop. Simple and inexpensive amplification can be obtained using an MECL-III quad line receiver (see Section III), which has a maximum voltage amplification of a factor of 4 per gate, or a total of 256. The maximum output level is 1 V; hence the input level to the amplifier should be 5 mV or better. This dictates a maximum insertion loss of 46 dB. This requirement rules out quartz as the substrate, since this gives at best an insertion loss of 57 dB. Therefore, in the remainder of this section we eliminate quartz from further consideration and refer to $LiNbO_3$ only.

The 4-channel transducer as shown in Fig. 5(b) was deposited on $LiNbO_3$ and analyzed experimentally using a network analyzer. Results showed that each transducer could be represented by a series circuit consisting of a capacitance $C = 24$ pF, a resistance $R = 20\ \Omega$, and a small inductance $L = 5$ nH. Using the transducer capacitance of 24 pF and a finger resistance of 19 Ω (the radiation impedance at 220 MHz is 1 Ω) in the crossed-field equivalent circuit model, the insertion loss versus frequency for each channel was computed and compared with the experimentally observed values, Fig. 8. The agreement is fairly good. Near midband, the minimum computed insertion loss is 35 dB, which is 5 dB higher than the preceding loss mentioned. The difference is a result of a resistive loss of 19 Ω in the aluminum fingers, which accounts for 3 dB, and a capacitive reactance of 30 Ω instead of 50 Ω, which accounts for 2 dB. The 3-dB difference between the theoretical minimum and the experimental minimum in the insertion loss is presumed to be due to attenuation, diffraction, and beam walkoff, whose effects are not taken into account in the theory. The minimum observed insertion loss in the frequency domain is 37 dB, which yields an insertion loss in the time domain of 40 dB. Fig. 9 shows the experimentally observed delayed pulse. The shape of the pulse is in excellent agreement with the theoretically computed pulse shape as shown in Fig. 6. The time between input and output is 5.7 μs, and the insertion loss equals 40 dB, as computed. Cross talk between channels could be observed, but was more than 25 dB down compared to the delayed pulse. This was due mainly to direct leakage between input leads. Direct leakage from input to output transducer was so small it could not be observed. The delay line was also tested with a 16-bit word generator, Fig. 10. The upper trace on each photograph represents the clock; the lower trace shows various sequences of delayed pulses. In all cases, the ratio of a -1- to a -0- was 2:1 or better, which is a sufficiently large detection margin.

As is well known, there are two effects which may distort the delay line output, acoustic regeneration and transducer tap reflections. The first effect occurs when the driving voltage at the input transducer is perturbed by the acoustic wave which is launched by the driving voltage, and also when the voltage at the output transducer generates a secondary wave which in turn perturbs the output voltage. This effect is strongly dependent on the strength of the coupling factor and

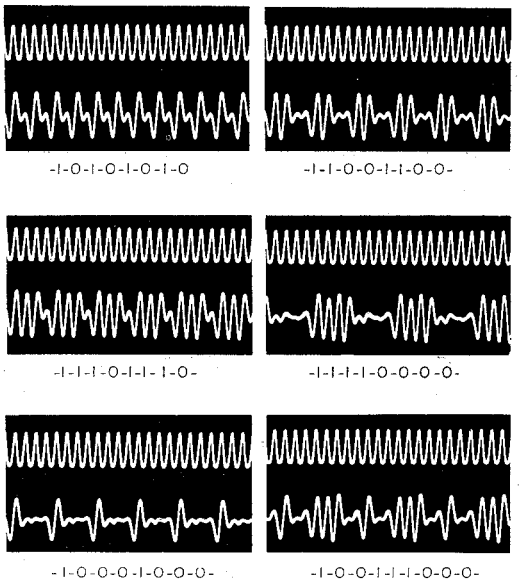

Fig. 10. Various pulse sequences as observed at output of delay line. Upper trace on each photograph represents clock signal.

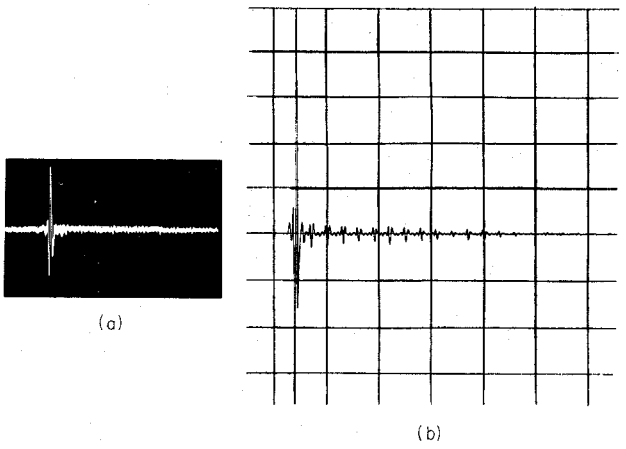

Fig. 11. Computed time response using the in-line model (a) and experimentally observed delayed pulse (b) of 16-bit Golay coded transducer pair on $LiNbO_3$.

on the source and load impedances. However, Speiser and Whitehouse have shown that Golay coded or other complementary transducers in parallel generate identically canceling perturbation voltages, and no acoustic regeneration occurs [11]. On the other hand, both mechanical and electromechanical reflections do occur and cause a series of reflections which are trailing the main correlation peak. Mechanical reflections are due to the mass loading of the aluminum fingers and a change in propagation velocity under the fingers. Electromechanical reflections are due to an effective change in mechanical impedance as a result of the piezoelectric coupling, and thus their magnitudes are dependent on the strength of the coupling factor.

Theoretically, the electromechanical reflections are contained only in the in-line model and not in the crossed-field model. The experimentally observed delayed pulse and the trailing tap reflections on $LiNbO_3$ are shown in Fig. 11(a). The reflections are down by 26 dB or more. The computed time response of the same 16-bit Golay code using the in-line model is shown in Fig. 11(b), with the maximum reflection

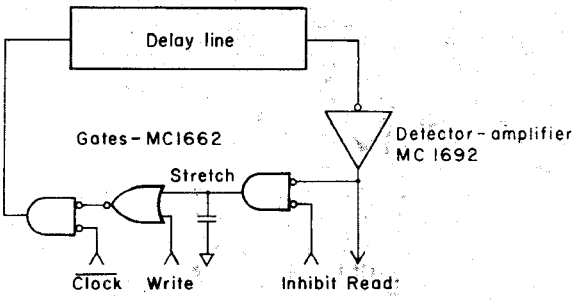

Fig. 12. Block diagram of recirculating electronics.

down by 26 dB from the main peak! The agreement between experiment and theory is perfect. These results seem to contradict the generally held belief that the crossed-field model is the better model to use in evaluating transducers on $LiNbO_3$. However, the results mentioned here are not conclusive, since the same results as shown in Fig. 11(b) could have been obtained using the crossed-field model and introducing mechanical reflections from the taps by assuming different acoustic impedances for the metallized and unmetallized portions of the transducer. For the present purpose, they can be omitted from further consideration because of their small amplitude.

III. Design of the Recirculating Electronics

The block diagram of the recirculating electronics shown in Fig. 12 follows closely that of Heiter [9]. However, in implementing this block diagram, first consideration was given to using immediately available commercial parts. Thus, the detector–amplifier, which raises the delay line output to logic levels, uses a standard Motorola MC1692 quad line receiver. A line receiver provides a broad-band voltage gain of 3 to 4 with good dc balance at a relatively low cost. Its chief disadvantage is that the four line receivers in one package tend to interact through the power connection, which are common to all four. In a four-channel recirculating memory, however, this can be overcome by using one package for the low-level stages of all four channels, thus keeping high-level pulses out of the input stages.

If production quantities warrant, it would not be difficult to produce a detector–amplifier circuit which would have fully differential coupling in the first three stages with the power supply connections to these stages brought out to pins for decoupling. This would provide higher gain and greater noise immunity than is available from the standard MC1692 without requiring any process changes.

Standard MECL-III two input gates (MC1662) are used to inhibit recirculation and to write new information. Pulse stretching is provided by capacitor loading at a gate output where the pulses are positive-going, such as the output of the inhibit gate.

The pulse shape at the output of the delay line changes very little with changes in driving waveshape. Thus, reclocking and reshaping are unnecessary in a single-channel store or a multichannel store where the channels are asynchronous. A single channel of the four-channel delay line has in fact been run successfully with the pulse stretcher and reclocking disabled.

The recirculating electronics was originally designed with a delay line driver amplifier using two discrete microwave transistors. This gave an output pulse of about 5-V amplitude which produced a delay line output pulse of about 50 mV.

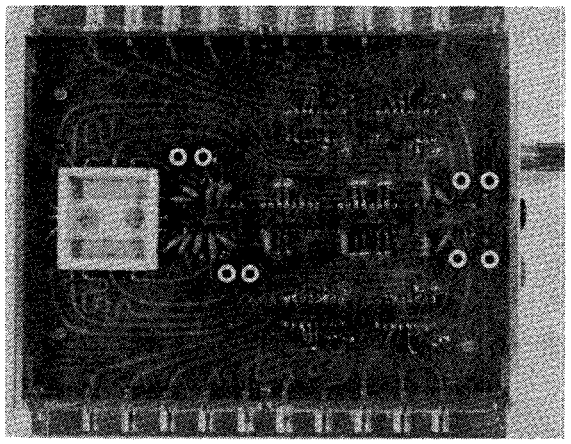

Fig. 13. Breadboard model of complete 4-channel 5000-bit recirculating memory.

For increased economy, however, it was decided to try driving the delay line directly from a MECL-III gate, which gave a delay line output of 8 mV. The lines were successfully operated in this mode, but since detailed margin studies have not yet been undertaken, it is not yet known whether this will give sufficient operating margin, especially against level shifts with temperature in the input stage of the detector–amplifier.

Bias shifts due to temperature changes in the input amplifier might be expected to amount to less than 50 μV/°C, or about $\pm$1-mV shift for $\pm$20°C temperature change. This is not unreasonable for an 8-mV pulse height, but noise and crosstalk margins must also be considered. The margins can be relieved by a factor of 2 by driving the input transducer differentially from a gate which has both inverting and noninverting outputs, which doubles the effective drive pulse and will thus yield 16-mV output.

A breadboard model of a four-channel 1280 bit-per-channel acoustic surface-wave memory, including the recirculation electronics, is shown in Fig. 13. All four channels can be run completely independently. The delay line itself is mounted inside a flatpack, hermetically sealed to prevent deterioration of the aluminum fingers. The microstrip lines of the four channels were made of equal length in order to reduce the amount of pulse stretching and reclocking when the lines were run in parallel. The total package measures 5 by 6 in, but this can probably be reduced by more careful design of the circuit layout. The various clock and inhibit pulses were provided by a separate circuit, which in turn was driven by a high-speed 16-bit word generator.

IV. Discussion and Conclusion

In this paper, we have reported a first attempt to utilize the acoustic surface-wave technology in the construction of a high-speed digital recirculating memory. $LiNbO_3$ was used as the delay material, primarily because of its high coupling constant and low propagation loss characteristics at frequencies of several hundred megahertz. However, it is well known that $LiNbO_3$ is temperature sensitive; its propagation velocity decreases with increasing temperature [19]. For many applications, this may not pose a problem. Techniques are well known where the clock signal is derived from or synchronized with the delay time; when the delay time varies, so does the clock frequency, in order to keep the clock in step with the bit rate. This, of course, increases the complexity of the system. In applications where temperature stability is required, $LiNbO_3$ cannot be used. As was already pointed out in Section II, the coupling constant of *ST* quartz, which has a zero temperature coefficient around room temperature [20] is too low, resulting in a too high insertion loss. A solution might possibly be found in using thin overlays of high coupling materials such as ZnO on substrates with low or zero temperature coefficients, such as *T*-40 glass.

As was mentioned in Section II, the measured insertion loss of the Golay coded delay line was 40 dB. This is somewhat high. Even though the memory could be operated with an amplifier input level of 8 mV, this level should be at least 30 mV for an acceptable detection margin [7]. This is equivalent to an insertion loss of 30 dB. It is expected that, by proper redesign of the transducer and using thicker aluminum fingers to obtain lower conduction losses, the insertion loss can be reduced by ~5 dB. The remaining 5 dB can be obtained by using nonpiezoelectric overlays over the transducers; a 71-percent increase in $\Delta V/V$ was recently reported for gallium arsenide on $LiNbO_3$ [21]. However, one has to be aware that any overlay causes dispersion, which may cause severe pulse distortion.

Finally, a paper on any memory is incomplete without a discussion on the cost per information bit. The following analysis of the cost of the acoustic surface-wave memory is very crude and is restricted to materials and electronics cost only. First, consider the electronics. In the simple configuration shown in Fig. 12, where the data can be read out serially only, the recirculation electronics consists of two standard MECL-III dual in-line packages only, one MC1662L and one MC1692L, each of which costs $7.50 in lots of 100 at current prices, plus a circuit board and some assorted capacitors and resistors. Assuming that power supplies, clock generators, etc., will be shared by many parallel running memories, it is not unreasonable to estimate the cost of the electronics per channel to be less than $20. As far as the delay material is concerned, the cost of $LiNbO_3$, which was used as the substrate material in the memory reported here, has come down rapidly during the past few years. A price of $6 per centimeter of polished substrate was recently reported [22]. This would make the cost of the delay material used here $3 per channel (2-cm substrate, 4 channels). Total: ~$23 for 1280 bit, or 1.8 ¢/bit, not counting manufacturing cost. This is high. It is interesting to note, however, that the cost is dominated by the electronics and not by the substrate material. The key to reducing the cost is obviously to increase the number of bits per channel served by one recirculation loop. In the present configuration, it is estimated that the length of the delay line can be increased by a factor of 2 to 3 without increasing the total insertion loss too much. Thus, with essentially the same electronics the cost would reduce to less than 1¢/bit. Reducing the bit rate to ~100 MHz instead of 200 MHz decreases the storage capacity. On the other hand, at such a bit rate the slower MECL 10 000 can be used, which at present is roughly four times cheaper than MECL-III. Thus, the same 1280 bit per channel would require a 4-cm-long substrate, or $6 per channel, but the electronics would be ~$5 per channel, or 0.9¢/bit, not counting manufacturing cost.

These costs must be compared to costs of other possible memory technologies. For example, large relatively slow core memories cost on the order of 1¢/bit, and this is for a complete memory system with random access. Magnetic bubble domain memories and charge-coupled semiconductor memories, both organized as shift registers, are projected to cost

less than 0.1¢/bit in large quantities. Current price lists show costs of a little less than 0.8¢/bit for LSI shift registers in single quantities. The acoustic surface-wave memory discussed here cannot compete with such costs per bit, unless the very high data rates possible with the surface-wave technology are critical to the application.

A large reduction in cost is possible if storage times in the order of several hundred microseconds can be obtained. Recently, delay times up to several milliseconds at frequencies up to 100 MHz were reported [23]. These delay lines use bismuth germanium oxide, and the surface waves are circulated around the periphery of the sample in multiple turns (wrap-around delay lines). Internal amplification is used to overcome the propagation losses, principally associated with the rounded edges. Estimates indicate that such a memory could easily contain 100 000 bit in one channel, and that it should be possible to make such a device and its recirculation electronics for $50, or 0.05¢/bit. This cost approaches that of a rotating magnetic memory, but with an order of magnitude smaller latency time. It might thus find a place in the memory hierarchy similar to drums and disks. However, the problem of surface-wave dispersion introduced by the internal amplifier must be thoroughly investigated. If the dispersion can be kept acceptably low, surface acoustic wave delay lines show good promise in memories with high capacity, high data rates, and low cost.

Acknowledgment

The authors wish to thank the expert technical assistance of R. A. St. Cyr in both the circuit layout and the construction of the delay line.

References

[1] B. G. Starr, "Low cost data storage with ultrasonic delay lines," *Ultrasonics*, vol. 3, pp. 188–189, Oct./Dec. 1965.
[2] R. E. Mattik, "Review of current proposed technologies for mass storage systems," *Proc. IEEE*, vol. 60, pp. 266–289, Mar. 1972.
[3] J. H. Eveleth, "A survey of ultrasonic delay lines operating below 100 Mc/s," *Proc. IEEE*, vol. 53, pp. 1406–1428, Oct. 1965.
[4] A. H. Meitzler, "Ultrasonic delay lines for digital data storage," *IRE Trans. Ultrason. Eng.*, vol. UE-9, pp. 30–37, Dec. 1962.
[5] E. K. Sittig and F. M. Smits, "Recirculating ultrasonic stores: An economical approach to sequential storage with bit rates beyond 100 MHz," *Bell Syst. Tech. J.*, vol. 48, pp. 659–674, Mar. 1969.
[6] F. M. Smits and E. K. Sittig, "Ultrasonic digital storage, present and future," *Ultrasonics*, vol. 7, pp. 167–170, July 1969.
[7] E. K. Sittig, "High-speed ultrasonic digital delay line design. A restatement of some basic considerations," *Proc. IEEE*, vol. 56, pp. 1194–1202, July 1968.
[8] G. L. Heiter and E. H. Young, Jr., "A 100 MHz, 1024-bit, recirculating ultrasonic delay-line store," *ISSCC Dig. Tech. Papers*, paper 10.3, Feb. 1968.
[9] G. L. Heiter, "100-MHz 1000-bit ultrasonic digital delay-line time-compression store," *IEEE J. Solid-State Circuits*, vol. SC-6, pp. 61–71, Apr. 1971.
[10] A. N. Broers, E. G. Lean, and M. Hatzakis, "1.75 GHz acoustic surface wave transducer fabricated by an electron beam," *Appl. Phys. Lett.*, vol. 15, pp. 98–101, Aug. 1969.
[11] J. M. Speiser and H. J. Whitehouse, "Surface wave transducer array using transversal filter concept," in *Acoustic Surface Wave and Acousto-Optic Devices*. New York: Optosonic Press, 1971, pp. 81–90.
[12] C. C. Tseng, "Signal multiplexing in surface-wave delay lines using orthogonal pairs of Golay's complementary sequences," *IEEE Trans. Sonics Ultrason.*, vol. SU-18, pp. 103–107, Apr. 1971.
[13] W. R. Smith, H. M. Gerard, J. H. Collins, T. M. Reeder, and H. J. Shaw, "Analysis of interdigital surface wave transducers by use of an equivalent circuit model," *IEEE Trans. Microwave Theory Tech. (Special Issue on Microwave Acoustics)*, vol. MTT-17, pp. 856–864, Nov. 1969.
[14] H. Engan, "Excitation of elastic surface waves by spatial harmonics of interdigital transducers," *IEEE Trans. Electron Devices*, vol. ED-16, pp. 1014–1017, Dec. 1969.
[15] T. L. Szabo and A. J. Slobodnik, Jr., "The effect of diffraction on the design of acoustic surface wave devices," to be published.
[16] W. D. Squire, H. J. Whitehouse, and J. M. Alsup, "Linear signal processing and ultrasonic transversal filters," *IEEE Trans. Microwave Theory Tech.*, vol. MTT-17, pp. 1020–1040, Nov. 1969.
[17] E. K. Sittig, "Transmission parameters on thickness-driven piezoelectric transducers arranged in multilayer configurations," *IEEE Trans. Sonics Ultrason.*, vol. SU-14, pp. 167–174, Oct. 1967.
[18] R. H. Tancrell and M. G. Holland, "Acoustic surface wave filters," *Proc. IEEE*, vol. 59, pp. 393–409, Mar. 1971.
[19] J. D. Maines, E. G. S. Paige, A. F. Saunders, and A. S. Young, "Simple technique for the accurate determination of delay-time variations in acoustic-surface-wave structures," *Electron. Lett.*, vol. 5, pp. 678–680, Dec. 1969.
[20] M. B. Schultz and M. G. Holland, "Surface acoustic wave delay lines with small temperature coefficient," *Proc. IEEE* (Lett.), vol. 58, pp. 1361–1362, Sept. 1970.
[21] L. P. Solie, "Piezoelectric acoustic surface waves for a film on substrate," *Appl. Phys. Lett.*, vol. 18, pp. 111–112, Feb. 1971.
[22] L. J. Castelli, *Electronics*, p. 8, Sept. 27, 1971.
[23] T. M. Reeder, H. J. Shaw, and E. M. Westbrook, "Multimillisecond time delays with wrap-around surface-acoustic wave delay lines," *Electron. Lett.*, vol. 8, pp. 356–358, July 1972.